International Journal of Engineering Research and Technology. ISSN 0974-3154, Volume 13, Number 12 (2020), pp. 4693-4700

The Effects of Large Vibration Amplitudes on the non Linear Free and Forced Response of Fully Clamped Functionally Graded Skew Plates

H. Moulay Abdelali[1] and R.Benamar[2]

[1,2]Mohammed V University in Rabat- Ecole Mohammadia D'ingénieurs, Avenue Ibn Sina, B.P.765, Agdal, Rabat, Morocco.

Abstract

The present work concerns the geometrically non-linear forced vibration of fully clamped functionally graded skew plates (FGSP). The functionally graded materials possess the best qualities of their constituents, i.e. strength and toughness from the metal and excellent heat resistance from the ceramic. The theoretical model based on Hamilton's principle and spectral analysis previously applied to obtain the non-linear mode shapes and resonance frequencies of thin straight structures, such as beams, plates and shells is used. A homogenization technique has been developed to reduce the FGSP problem under consideration to that of an isotropic homogeneous skew plate. The material properties of the skew plate examined herein are assumed to be graded in the thickness direction of the plate according to the power-law distribution in terms of volume fractions of the constituents. Results are given for the linear and non-linear fundamental frequency and associated mode shape of fully clamped FGSP, considering different parameters such as the skew angle, the intensity of the excitation force, the vibration amplitude and the plate aspect ratio. The results showed, as may be expected due to the membrane forces induced by the large vibration amplitudes, a non linearity of the hardening type with a shift to the right of the bent frequency response function, in the neighborhood of the fundamental mode. Also, the hardening effect is more accentuated for FGSP than that obtained for similar homogeneous plates. The effects of the various parameters mentioned above have been examined and the comparison between the results obtained and those available in previous studies showed a good agreement.

Keywords Non-linear vibrations, FGM skew plate, Homogenization technique, Forced vibration, Stress.

I. INTRODUCTION (12 BOLD)

Classical composite materials are used in many industrial fields but may not be appropriate for use under high-temperature conditions. The functionally graded materials possess the best qualities of their constituents, i.e. strength and toughness from the metal and excellent heat resistance from the ceramic. Since these materials are non homogeneous, they offer a possible decrease in the in-plane and through-the thickness transverse stresses in addition to the improved thermal behavior owing to low thermal conductivity of the ceramic component. The FGM are actually used in various fields such as medicine, civil engineering, aeronautic and aerospace. The vibration of rectangular FG plates has been investigated by many researchers but the nonlinear vibrations of FGSP have been less investigated. Fazzolari and Carrera [1] developed a fully coupled thermo-elastic formulation to deal with the free vibration analysis of anisotropic composite plates and isotropic/sandwich FG plates. The thermo-elastic coupling was investigated in terms of natural frequencies and the effect of stacking sequence and length-to-thickness ratio for lower and higher modes was discussed. Zhang, and Zhou [2] presented a theoretical analysis of FG thin plates, based on the physical neutral surface. The physical neutral surface of a FG plate was determined by the classical thin plate theory in an easy way, similar to that generally used for homogeneous isotropic plates; the validity of this theory was verified by comparison with related publications. Belabed and his co-author [3] presented an efficient and a simple higher order shear and normal deformation theory for FG plates. By dividing the transverse displacement into bending, shear and thickness stretching parts, the number of unknowns and governing equations was reduced, significantly facilitating the engineering analysis especially for predicting simply the bending and the free vibration response of FG plates. Prakash, Singha and Ganapathi [4] investigated the large flexural vibration amplitude characteristics of FG plates using a shear flexible finite element approach. The non-linear equations of motion were solved using Newmark's time integration technique. This work was dealing with the non-linear flutter characteristics of FG plates under high supersonic airflow accounting for both the geometric and aerodynamic non-linearities. Dinh Duc and Hong Cong [5] presented an analytical investigation on the nonlinear post buckling of imperfect eccentrically stiffened thin FG plates under a temperature effect and resting on elastic foundations using a simple power-law distribution (P-FGM). The formulation was based on the classical plate theory taking into account the geometrical nonlinearity, the initial geometrical imperfection, temperature-dependent properties and the Lekhnitsky smeared stiffeners technique with Pasternak type elastic foundation. Birman and Byrd [6] presented a review of the principal developments in FGMs with an emphasis on the recent works published since 2000. Diverse areas relevant to various aspects of theory and applications of FGM were reflected in this paper. They included homogenization, heat transfer issues, stress, stability and dynamic analyses, testing, manufacturing and design applications, and fracture. The critical area where further research was needed for a successful implementation of FGM in design was outlined in the conclusions. Xia and Shen [7] studied nonlinear vibration

and dynamic response of a shear deformable FG plate with surface-bonded piezoelectric fiber reinforced composite actuators (PFRC) in thermal environments. The formulation was based on the higher order shear deformation plate theory and general von Kármán-type equations that include thermo-piezoelectric effects. The results revealed that the effect of control voltage on the natural frequency of an FG plate with PFRC actuators is larger than that of the plate with monolithic piezoelectric actuators. Sundararajan, Prakash and Ganapathi [8] studied the free vibration characteristics of FG rectangular and skew plates subjected to thermal environment. The effective material properties were estimated from the volume fractions and the material properties of the constituents using Mori–Tanaka homogenization method. The nonlinear governing equations obtained using Lagrange's equations of motion were solved using the finite element procedure coupled with the direct iteration technique. The results obtained revealed that the temperature field and gradient index have significant effect on the nonlinear vibration of the FG plate. Boukhzer et al [9] presented a homogenization technique for the non-linear free vibrations analysis of FG rectangular plates. A homogenization technique has been developed to reduce the FGRP problem under consideration to that of an isotropic homogeneous rectangular plate. The theoretical model proposed was based on the classical plate theory and the Von Karman relationships, and the amplitude equation was derived in the form of a set of non-linear algebraic equation using Hamilton's principle and a multimode approach. Jaberzadeh et al [10] investigated the thermal buckling of functionally graded skew and trapezoidal plates using the free element Galerkin method. The effects of the aspect and thickness ratios, the gradient index and the skew angle on the critical buckling temperature difference were examined. This research showed that the EFG method is very efficient computationally and constitutes a very simple procedure for modeling skew and trapezoidal plates with various boundary conditions. Upadhyay and Shukla [11] presented geometrically nonlinear static and dynamic analyses of FGSP. Higher order shear deformation theory and von-Karman's nonlinearity were considered in the problem formulation. The post-buckling response of skew plates was investigated for different types of in-plane compressive loadings. The effects of the skew angle, the lamination scheme, the core thickness and the face to core material property ratio of the sandwich plate on the buckling and Post buckling response have been studied in detail. The effect of transverse shear was observed for highly skewed plates. Geometrically non-linear free and forced vibration of fully clamped FGSP is examined here using a homogenization technique, in order to investigate the effect of non-linearity on the amplitude dependent non-linear resonance frequency and associated non-linear fundamental mode shape at large vibration amplitudes. The non-linear resonance frequency ratio ωnl/ωl is determined for various values of the plate skew angle and a wide range of vibration amplitudes. Large deflection responses of functionally graded rectangular plates under transverse loads is investigated by using a semi-analytical approach and compared with previous results.

II.GEOMETRICALLY NON-LINEAR VIBRATION OF FULLY CLAMPED FGSP

II.1. Constitutive Equation of a FGSP at Large Deflections

Consider the FGSP shown in Fig. 1 with a skew angle θ and a plate thickness H. Metal and ceramics are the two isotropic materials constituting the skew plate, with a composition varying from the plate top surface (Z=H/2), which is ceramic rich, to the bottom surface (Z=-H/2), which is metal rich. The plate thickness is considered to be sufficiently small so as to avoid the effects of shear deformation. The skew plate has the following characteristics: a, b, S: length, width and area of the plate; x-y: plate co-ordinates in the length and the width directions; ξ-η: Skew plate co-ordinates.

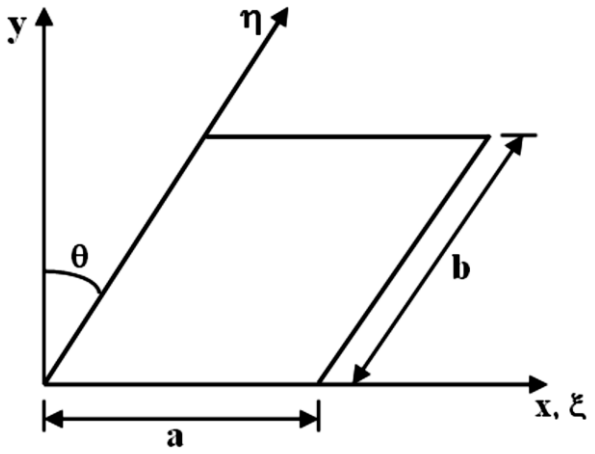

Fig.1. FGSP in x-y and ξ-η co-ordinate system

The elastic material properties vary through the plate thickness according to the volume fractions of the constituents. The variation of material properties is described by a Power-law distribution expressed as:

$$P(z) = (P_c - P_m)V_c(z) + P_m \quad (1)$$

$$V_c(z) = \left(\frac{z}{h} + \frac{1}{2}\right)^n \ (0 \le n \le \infty) \quad (2)$$

Where P represent the material property, Pm and Pc represents the properties of the metal and ceramic, respectively; Vc is the volume fraction of the ceramic and n is the volume fraction exponent. The Young's modulus E and the mass density ρ vary according to Eq. 1 and Eq. 2 but Poisson's ratio ν is assumed to be constant. The power-law is used as a simple mixture rule to express the variation of the effective properties of the ceramic–metal in the thickness direction of the FGSP. The temperature is assumed to be equal to 300 (° K) and the materials used are Zirconia (ZrO2) on the top and aluminum on the bottom. The Young's modulus and mass density are given in Table 1.

Table 1: Material properties of the metal and ceramic constituents of the FGSP.

Material	E (GPa)	ρ (Kg/m^3)	ν
Ceramic (Zirconia)	151	3000	0.3
Metal (Aluminum)	71	2707	0.3
Ti-6Al-4V (Titanium)	122	4512	0.28

Consider transverse vibrations of the plate shown in fig 1. From the classical plate theory, the strain-displacement relationships at large deflections are given by:

$$\{\varepsilon\} = \{\varepsilon^0\} + z\{k\} + \{\lambda^0\} \tag{3}$$

In which $\{\varepsilon^0\}$, $\{k\}$ and $\{\lambda^0\}$ are respectively the column matrix of strains due to the in-plane displacements u, v, w, the column matrix of bending or twisting and the column matrix of strains induced by large displacements W given by:

$$\{\varepsilon^0\} = \begin{bmatrix} \frac{\partial U}{\partial x} \\ \frac{\partial V}{\partial y} \\ \frac{\partial U}{\partial y} + \frac{\partial V}{\partial x} \end{bmatrix}. \{k\} = \begin{bmatrix} k_x \\ k_y \\ k_{xy} \end{bmatrix} = \begin{bmatrix} \frac{-\partial^2 W}{\partial x^2} \\ \frac{-\partial^2 W}{\partial Y^2} \\ \frac{-2\,\partial^2 W}{\partial xy} \end{bmatrix}. \{\lambda^0\} = \begin{bmatrix} \lambda_x^0 \\ \lambda_y^0 \\ \lambda_{xy}^0 \end{bmatrix} = \begin{bmatrix} \frac{1}{2}\left(\frac{\partial W}{\partial x}\right)^2 \\ \frac{1}{2}\left(\frac{\partial W}{\partial y}\right)^2 \\ \frac{\partial W}{\partial x}\frac{\partial W}{\partial y} \end{bmatrix} \tag{4-6}$$

U, V and W are the displacements of the plate mid-plane, in the x, y and z directions respectively. The stresses can be expressed as:

$$\{\sigma\} = [Q]\{\varepsilon\} \tag{7}$$

In which $\{\sigma\}^T = [\sigma_x \sigma_y \sigma_{xy}]$ and the terms of the matrix [Q] of transformed stiffness can be obtained by:

$$[Q] = \frac{E(z)}{1-\nu^2}\begin{bmatrix} 1 & \nu & 0 \\ \nu & 1 & 0 \\ 0 & 0 & \frac{1-\nu}{2} \end{bmatrix} \tag{8}$$

The in-plane forces N and bending moments M in the plate are given by:

$$\begin{bmatrix} N \\ M \end{bmatrix} = \begin{bmatrix} A & B \\ B & D \end{bmatrix}\begin{bmatrix} \{\varepsilon^0\} + \{\lambda^0\} \\ \{k\} \end{bmatrix} \tag{9}$$

A, B and D are the extensional, coupling and bending stiffness coefficients given in term of symmetric matrices by Eq. 10.

$$(A_{ij}, B_{ij}, D_{ij}) = \int_{-H/2}^{H/2} Q_{ij}(1, z, z^2)\, dz \tag{10}$$

Here the Q_{ij} are the reduced stiffness coefficients in the plate co-ordinates. The axial displacements u and v are neglected considering the analysis made in reference [13]. The expression for the bending strain energy Vb, the membrane strain energy Vm, the coupling strain energy Vc and the kinetic energy T are given in rectangular coordinate in reference [9]. The skew co-ordinates are related to the rectangular co-ordinate (ξ,η) by: ξ=x-y tanθ ; η=y/cosθ. So, the strain energy due to bending Vb, the membrane strain energy Vm, the coupling strain energy Vc and the kinetic energy T are given below. In order to simplify the expressions and reduce the problem to that of a homogeneous skew plate, the change of variable z1=z-c is made, With $c = \frac{B_{11}}{A_{11}}$. Consequently, the coupling term Vc vanishes and the bending strain and the membrane strain energy expressions are written in the ξ-η co-ordinate system as:

$$V_b = \frac{D_{11}A_{11} - {B_{11}}^2}{2A_{11}} \int_A \left[\frac{1}{\cos^4\theta}\left(\frac{\partial^2 w}{\partial \xi^2} + \frac{\partial^2 w}{\partial \eta^2} - 2\sin\theta \frac{\partial^2 w}{\partial \xi\, \partial \eta}\right)^2 + \frac{2(1-\nu)}{\cos^2\theta}\left(\left(\frac{\partial^2 w}{\partial \xi\, \partial \eta}\right)^2 - \left(\frac{\partial^2 w}{\partial \xi^2}\frac{\partial^2 w}{\partial \eta^2}\right)\right)\right] dA \tag{11}$$

$$V_a = \frac{A_{11}}{8} \int_A \left[\frac{1}{\cos^4\theta}\left(\left(\frac{\partial w}{\partial \xi}\right)^2 + \left(\frac{\partial w}{\partial \eta}\right)^2 - 2\sin\theta \frac{\partial^2 w}{\partial \xi\, \partial \eta}\right)^2 \right] dA \tag{12}$$

$$T = \frac{1}{2} \int_{-H/2}^{H/2} \rho(z) dz. \int_A \left(\frac{\partial w}{\partial t}\right)^2 dA \tag{13}$$

Where: dA=cosθ dξdη and W (ξ, η, t) is the transverse displacement function.

II.2 Numerical Model for the Non-Linear Mode Shapes and Resonance Frequency of Fully Clamped FGM Skew Plates

The FGSP transverse displacement function W may be written as in references [9] in the form of a double series:

$$W = \{A_k\}^T \{W\} \sin k\omega t \tag{14}$$

Where $\{A_k\}^T = \{a_1^k, a_2^k, \dots, a_n^k\}$ is the matrix of coefficients corresponding to the kth time harmonic, $\{W\}^T = \{w_1, w_2, \dots, w_n\}$ is the basic spatial functions matrix, k is the number of harmonics taken into account, and the usual summation convention on the repeated index k is used. As in reference [9], only the term corresponding to k=1 has been taken into account, which has led to the displacement function series reduced, to only one harmonic: i.e.,

$$W = a_i\, w_i(x, y) \sin\omega t \tag{15}$$

Here, the usual summation convention for the repeated indices i is used. The index i is summed over the range 1 to n, with n being the number of basic functions considered. The discretization of the strain and kinetic energy expressions can be carried out, leading to:

$$V_b = \frac{1}{2}\sin^2(\omega t) a_i a_j k_{ij}.\ V_a = \frac{1}{2}\sin^4(\omega t) a_i a_j a_k a_l b_{ijkl}.\ T = \frac{1}{2}\omega^2 \cos^2(\omega t) a_i a_j m_{ij} \tag{16-18}$$

In which mij, kij and bijkl are the mass tensor, the rigidity tensor and the geometrical non-linearity tensor respectively. The expressions for these tensors are:

$$k_{ij} = \frac{D_{11}A_{11}-B_{11}{}^2}{2A_{11}} \cdot \frac{1}{\cos^3\theta} \int_A^{\circ} \left[\frac{\partial^2 w_i}{\partial \xi^2}\frac{\partial^2 w_j}{\partial \xi^2} + \frac{\partial^2 w_i}{\partial \eta^2}\frac{\partial^2 w_j}{\partial \eta^2} + \frac{\partial^2 w_i}{\partial \xi^2}\frac{\partial^2 w_j}{\partial \eta^2} + \right.$$

$$\frac{\partial^2 w_i}{\partial \eta^2}\frac{\partial^2 w_j}{\partial \xi^2} - 2\sin\theta \left(\frac{\partial^2 w_i}{\partial \xi^2}\frac{\partial^2 w_j}{\partial \xi\,\partial \eta} + \frac{\partial^2 w_i}{\partial \eta^2}\frac{\partial^2 w_j}{\partial \xi\,\partial \eta} + \frac{\partial^2 w_i}{\partial \xi\,\partial \eta}\frac{\partial^2 w_j}{\partial \xi^2} + \right.$$

$$\left. \frac{\partial^2 w_i}{\partial \xi\,\partial \eta}\frac{\partial^2 w_j}{\partial \eta^2} \right) + 4\sin^2\theta \frac{\partial^2 w_i}{\partial \xi\,\partial \eta}\frac{\partial^2 w_j}{\partial \xi\,\partial \eta} + 2(1-\nu)\cos^2\theta \left(\frac{\partial^2 w_i}{\partial \xi\,\partial \eta}\frac{\partial^2 w_j}{\partial \xi\,\partial \eta} - \right.$$

$$\left. \left. \frac{\partial^2 w_i}{\partial \xi^2}\frac{\partial^2 w_j}{\partial \eta^2} \right) \right] d\xi d\eta \qquad (19)$$

$$b_{ijkl} =$$

$$\frac{A_{11}}{8} \cdot \frac{1}{\cos^3\theta} \int_A^{\circ} \left[\frac{\partial w_i}{\partial \xi}\frac{\partial w_j}{\partial \xi} + \frac{\partial w_i}{\partial \eta}\frac{\partial w_j}{\partial \eta} - 2\sin\theta \frac{\partial w_i}{\partial \eta}\frac{\partial w_j}{\partial \xi} \right] \left[\frac{\partial w_k}{\partial \xi}\frac{\partial w_l}{\partial \xi} + \right.$$

$$\left. \frac{\partial w_k}{\partial \eta}\frac{\partial w_l}{\partial \eta} - 2\sin\theta \frac{\partial w_k}{\partial \eta}\frac{\partial w_l}{\partial \xi} \right] d\xi d\eta \qquad (20)$$

$$m_{ij} = \rho H \cos\theta \int_A^{\circ} w_i\, w_j d\xi d\eta \qquad (21)$$

The non-dimensional formulation of the non-linear vibration problem has been carried out as follows.

$$w_i(\xi,\eta) = H w_i^*\left(\frac{\xi}{a},\frac{\eta}{b}\right) = H w_i^*(\xi^*,\eta^*) \qquad (22)$$

Where $\xi^*$and $\eta^*$are non-dimensional co-ordinates $\xi^* = \frac{\xi}{a}$ and $\eta^* = \frac{\eta}{b}$. One then obtains:

$$k_{ij} = \frac{aH^4A_{11}}{2b^3\cos\theta^3} k_{ij}^*. \quad b_{ijkl} = \frac{aH^4A_{11}}{2b^3\cos\theta^3} b_{ijkl}^*. \quad m_{ij} =$$

$$\int_{-H/2}^{H/2} \rho(z)dz.\, H^2 ab\cos\theta m_{ij}^* \qquad (23)$$

Where the non-dimensional tensors m*ij, k*ij and b*ijkl are given in terms of integrals of the non-dimensional basic function wi*. Upon neglecting energy dissipation, the equation of motion derived from Hamilton's principle is:

$$\delta \int_0^{2\pi} (V - T) = 0 \qquad (24)$$

Where V=Va+Vb. Insertion of Eq. 16, Eq. 17 and Eq. 18 into Eq. 26, and derivation with respect to the unknown constants ai, leads to the following set of non-linear algebraic equations:

$$2a_i k_{ir}^* + 3a_i a_j a_k b_{ijkr}^* - 2\omega^* a_i m_{ir}^* = 0, \quad r=1\ldots n \qquad (25)$$

These have to be solved numerically. To complete the formulation, the procedure developed in reference [13] is adopted to obtain the first non-linear mode. As no dissipation is considered here, a supplementary equation can be obtained by applying the principle of conservation of energy, which can be written as:

$$V_{max} = T_{max} \qquad (26)$$

This leads to the equation:

$$\omega^{*2} = \frac{a_i a_j k_{ij}^* + (3/2) a_i a_j a_k a_l b_{ijkl}^*}{a_i a_j m_{ij}^*} \qquad (27)$$

This expression for ω*2 is substituted into Eq. 37 to obtain a system of n non-linear algebraic equations leading to the contribution coefficients ai, i=1 to n. ω and ω* are the non-linear frequency and the non-dimensional non-linear frequency parameters related by:

$$\omega^2 = \frac{D}{\rho b^4 \cos^4\theta} \omega^{*2} \qquad (28)$$

To obtain the first non-linear mode shape of the skew plate considered, the contribution of the first basic function is first fixed and the other basic functions contributions are calculated via the numerical solutions of the remaining (n-1) non-linear algebraic equations.

In this section, a fully clamped laminate skew plate excited by a concentrated harmonic force Fc applied at the point (ξ0,η0); or by a distributed harmonic uniform force Fd, distributed over the surface of the plate S are considered. Fc and Fd may be written using the Dirac function δ as:

$$F^c(\xi,\eta,t) = F^c \delta(\xi - \xi_0)\delta(\eta - \eta_0)\sin\omega t \qquad (29)$$

$$F^d(\xi,\eta,t) = F^d \sin\omega t \text{ if } (\xi,\eta) \in S \qquad (30)$$

$$F^d(\xi,\eta,t) = 0 \text{ if } (\xi,\eta) \notin S \qquad (31)$$

The corresponding generalized forces Fic(t) and Fid(t) in the beam function basis (BFB) are given by:

$$F_i^c(t) = F^c w_i(x_0,y_0)\sin\omega t = f_i^c \sin\omega t \qquad (32)$$

$$F_i^d(t) = F^d \sin\omega t \int_\Omega w_i(x_0,y_0)\, dxdy = f_i^d \sin\omega t \qquad (33)$$

Adding the forcing term to the right hand side of equation (25) leads to:

$$2a_i k_{ir}^* + 3a_i a_j a_k b_{ijkr}^* - 2\omega^* a_i m_{ir}^* = f_r^*, r = 2,3,\ldots,18 \qquad (34)$$

Where f_i^{*c} and f_i^{*d} corresponding, respectively to the dimensionless generalized concentrated force Fc at point (ξ0,η0); and to the uniformly distributed force Fd over the surface Ω of the plate; The expressions obtained are:

$$f_i^{*c} = F^c \frac{b^3}{aEH^4} w_i^{*c}(\xi_0^*, \eta_0^*) \qquad (35)$$

$$f_i^{*d} = F^d \frac{b^4}{EH^4} \iint_\Omega w_i^*(\xi_0^*, \eta_0^*) \qquad (36)$$

II.3 Bending stress analysis

The bending stress associated to the fundamental non-linear mode shape was examined, which allows a quantitative understanding of the non-linearity effects. The maximum

bending strains $\varepsilon_{\xi b}$ and $\varepsilon_{\eta b}$ obtained are given by:

$$\varepsilon_{\xi b} = \frac{z}{2}\left(\frac{\partial^2 W}{\partial \xi^2}\right). \quad \varepsilon_{\eta b} = \frac{z}{2}\left(\frac{\partial^2 W}{\partial \eta^2}\frac{1}{\cos\theta} - \frac{2\tan\theta}{\cos\theta}\frac{\partial^2 W}{\partial \xi\,\partial \eta} + \frac{\partial^2 W}{\partial \xi^2}\tan^2\theta\right) \quad (37\text{-}38)$$

For the FGSP, the associated stresses $\sigma_{\xi b}$ and $\sigma_{\eta b}$ can be obtained by applying the plane stress Hooke's law as:

$$\sigma_{\xi b} = \frac{E(z).z}{2(1-\nu^2)}\left(\frac{\partial^2 W}{\partial \xi^2} + \nu\left(\frac{\partial^2 W}{\partial \eta^2}\frac{1}{\cos\theta} - \frac{2\tan\theta}{\cos\theta}\frac{\partial^2 W}{\partial \xi\,\partial \eta} + \frac{\partial^2 W}{\partial \xi^2}\tan^2\theta\right)\right) \quad (39)$$

$$\sigma_{\eta b} = \frac{E(z).z}{2(1-\nu^2)}\left(\frac{\partial^2 W}{\partial \eta^2}\frac{1}{\cos\theta} - \frac{2\tan\theta}{\cos\theta}\frac{\partial^2 W}{\partial \xi\,\partial \eta} + \frac{\partial^2 W}{\partial \xi^2}\tan^2\theta + \nu\frac{\partial^2 W}{\partial \xi^2}\right) \quad (40)$$

In terms of the non-dimensional parameters defined in the previous section, the non- dimensional stresses $\sigma^*_{\xi b}$ and $\sigma^*_{\eta b}$ are then given by:

$$\sigma^*_{\xi b} = z^*.\left(\alpha^2\frac{\partial^2 W^*}{\partial \xi^{*2}} + \nu\left(\frac{\partial^2 W^*}{\partial \eta^{*2}}\frac{1}{\cos\theta} - \alpha\frac{2\tan\theta}{\cos\theta}\frac{\partial^2 W^*}{\partial \xi^*\,\partial \eta^*} + \alpha^2\frac{\partial^2 W^*}{\partial \xi^{*2}}\tan^2\theta\right)\right) \quad (41)$$

$$\sigma^*_{\eta b} = z^*.\left(\frac{\partial^2 W^*}{\partial \eta^{*2}}\frac{1}{\cos\theta} - \alpha\frac{2\tan\theta}{\cos\theta}\frac{\partial^2 W^*}{\partial \xi^*\,\partial \eta^*} + \alpha^2\frac{\partial^2 W^*}{\partial \xi^{*2}}\tan^2\theta + \nu\alpha^2\frac{\partial^2 W^*}{\partial \xi^{*2}}\right) \quad (42)$$

The relationships between the dimensional and non dimensional stresses are:

$$\sigma = \frac{E(z)H^2}{2(1-\nu^2)b^2}\sigma^* \quad (43)$$

III. RESULTS AND DISCUSSION

The aim of this section is to apply the theoretical model presented above to analyze the geometrical non-linear free and forced dynamic response of fully clamped FGSP in order to investigate the effect of non-linearity on the non-linear resonance frequencies and non linear fundamental mode shape at large vibration amplitudes. Convergence studies were carried out, and the results are compared with those available from the literature through a few examples of FGSP. Calculation was made by using 18 functions corresponding to three symmetric beam functions in the ξ direction and three symmetric beam functions in the η direction, and three anti-symmetric beam functions in the ξ direction and three anti-symmetric beam functions in the η direction, which contribute significantly to the first non linear mode of the fully clamped skew plate. Table 2 shows the linear results for a fully clamped FG square plate for N=0 and skew angle θ=0° obtained using only 18 well-chosen plate functions. A good convergence is obtained.

Table 2 shows the linear results of a fully clamped FGSP for different values of volume fraction N and a skew angle θ=0° and an aspect ratio α=1. It can be noticed that the adimensional frequencies decreases with values of volume fraction N.

Table 2: Adimensional linear frequencies of fully clamped FGM square plate for different values of volume fraction N

N	**ω*linear**
0	64,20
0,5	57,71
1	52,78
2	46,10
5	35,09
10	26,94

Table 3 shows the adimensional nonlinear frequencies results of a fully clamped FGSP for different values of volume fraction N and different adimensional non-linear maximum displacement W*max . It can be noticed that the adimensional nonlinear frequencies ratio increase with values of volume fraction N and with adimensional non-linear maximum displacement W*max, it's hardening type of vibration.

Table 3: Adimensional nonlinear frequencies ratio of fully clamped FGM square plate for different values of volume fraction N and for different adimensional non-linear maximum displacement W*max

	ω*nl/ω*l					
W*max	**N=0**	**N=0,5**	**N=1**	**N=2**	**N=5**	**N=10**
0	1	1	1	1	1	1
0,2	1,0051	1,0063	1,0075	1,0098	1,0169	1,0285
0,4	1,0201	1,0249	1,0296	1,0387	1,0659	1,1095
0,6	1,0448	1,0551	1,0655	1,0851	1,1430	1,2328
0,8	1,0783	1,0961	1,1139	1,1470	1,2429	1,3871
1	1,1199	1,1466	1,1731	1,2219	1,3605	1,5633
1,2	1,1688	1,2054	1,2416	1,3076	1,4918	1,7547
1,4	1,2241	1,2715	1,3180	1,4022	1,6334	1,9570
1,6	1,2849	1,3436	1,4010	1,5040	1,7829	2,1671

Fig 2 shows the adimensional non-linear maximum displacement W*max of FG square plate (N=0, θ=0° and α=1) versus nonlinear frequency ratio. The comparison was made between the results obtained in reference [9] and the present results, and good agreement is noticed.

It can be seen that result from reference [9] was bigger than present result, because of the in plane displacement taken into the account in reference [9].

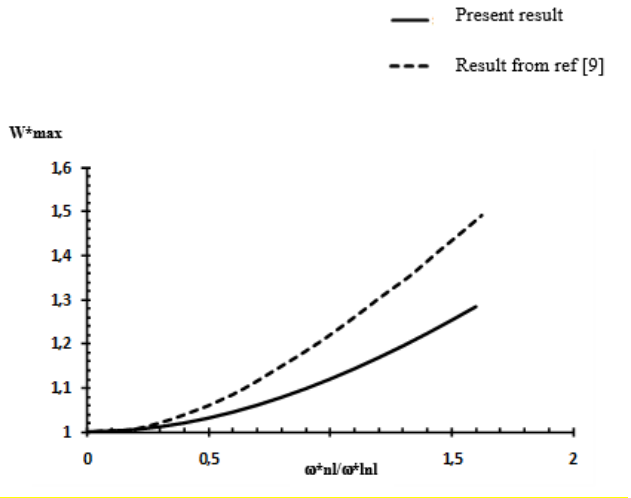

Fig.2. Adimensional non-linear maximum displacement W*max of FG square plate (N=0, θ=0° and α=1) versus nonlinear frequency ratio

Fig 3 shows the adimensional non-linear maximum displacement W*max of FG square plate (N=1, θ=0° and α=1) versus nonlinear frequency ratio. The comparison was made between the results obtained in reference [9] and the present results, and good agreement is noticed.

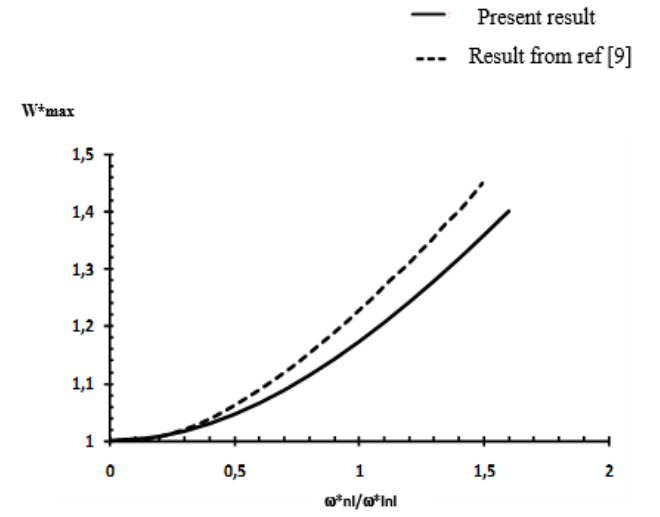

Fig. 3. Adimensional non-linear maximum displacement W*max of FG square plate (N=1, θ=0° and α=1) versus nonlinear frequency ratio

Fig 4 shows the adimensional non-linear maximum displacement W*max of FG square plate under uniform adimensional pressure $f_1{}^{*d}$ =100 in terms of the adimensional non linear frequency ratio and for different values of the volume fraction exponent. It can be seen that the non linearity increase with the volume fraction exponent. Fig 3 shows also the jump phenomena noted in the forced vibration.

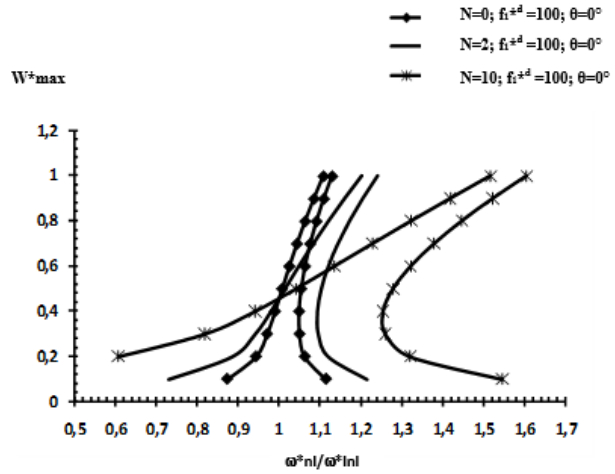

Fig.4. Effect of the volume fraction exponent on the vibration of fully clamped FGM square plate subjected to harmonic distributed force $f_1{}^{*d}$=100

Fig 5 shows the effect of the skew angle on the non linear vibration of fully clamped FGM skew plate subjected to harmonic distributed force $f_1{}^{*d}$=100 with a volume fraction exponent N=2. It can be seen that the nonlinearity decreased a little with the skew angle.

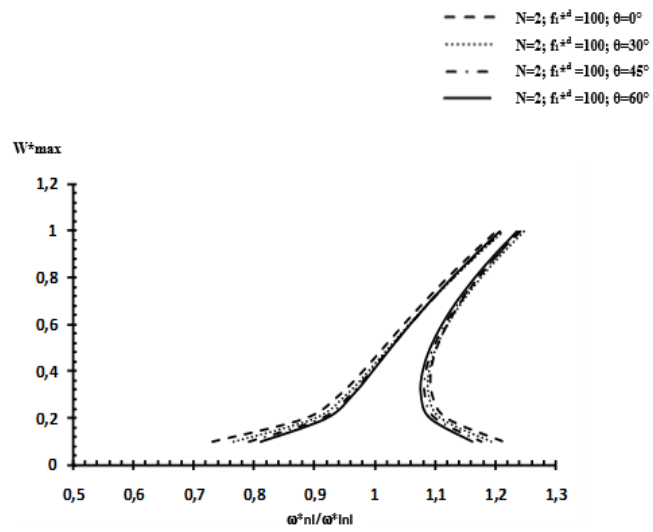

Fig.5. Effect of the skew angle on the non linear vibration of fully clamped FGM skew plate subjected to harmonic distributed force $f_1{}^{*d}$=100 with a volume fraction exponent N=2

Fig 6 shows the effect of the volume fraction exponent on the vibration of fully clamped FGM skew plate (θ=30°) subjected to harmonic distributed force $f_1{}^{*d}$=100. It can be seen that the nonlinearity increase with the volume fraction exponent.

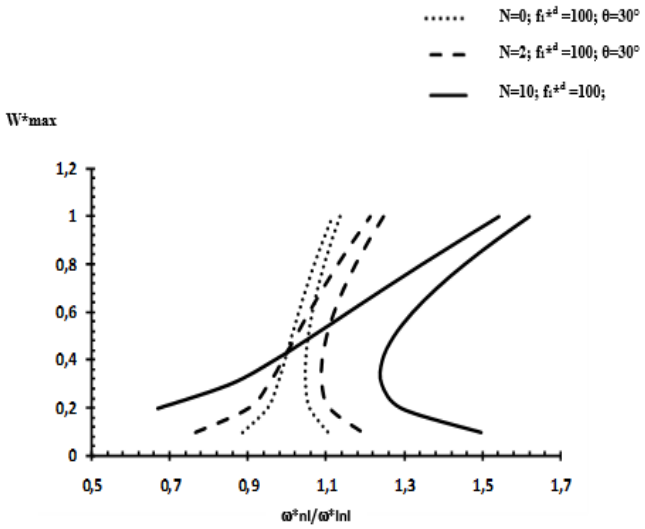

Fig.6. Effect of the volume fraction exponent on the vibration of fully clamped FGM skew plate (θ=30°) subjected to harmonic distributed force $f_1{}^{*d}$=100

The non-dimensional bending stress distribution associated with the FGSP first non-linear mode is plotted in Fig 7 and Fig 8 for the non-dimensional maximum amplitude vibration W^*_{max}=2 respectively for the case of a skew angle θ=30(°) and θ=45(°) and an aspect ratio α=0.6 along the section corresponding to η^*=0.5 and ξ^*=0.5 for different values of Z^*. It can be shown that the maximum value of the stress occurs at the centre of the top surface of the plate.

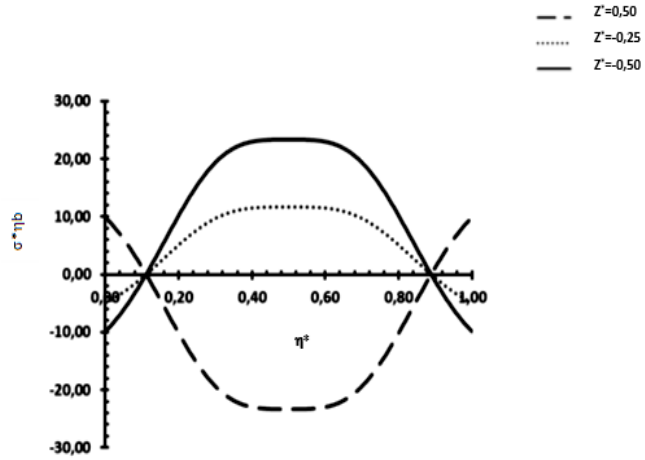

Fig. 7. Non-dimensional bending stress distribution associated with the fundamental non-linear mode of a fully clamped FGSP for θ=30(°) and α=0.6 for different edge surfaces for N = 2, T=300(° K) along the section ξ*=0.5.

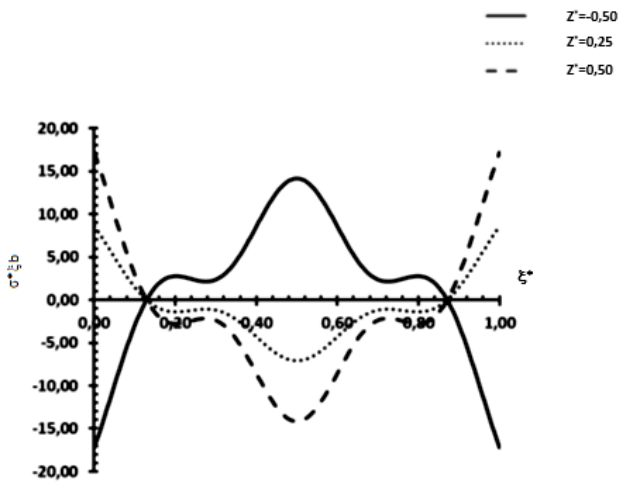

Fig. 8. Non-dimensional bending stress distribution associated to the fundamental non-linear mode of a fully clamped FGM skew plate for θ=45(°) and α=0.6 on different edge surfaces for N = 2, T=300(° K) along the section η*=0.5.

IV. CONCLUSION

The theoretical model established and applied to beams, plates and shells [13], has been successfully applied to calculate the first non-linear mode shape of fully clamped FGSP using the homogenization technique was applied for geometrical non-linear, steady state, periodic forced vibration of FGM skew plates for various volume fraction exponent and various skew angle. Static and dynamic response was investigated. The present formulation has been verified with the results available in the literature. The effect of the volume fraction index N, the skew angle θ has been discussed. Good results were found using a single and multimode approach to determine the amplitude frequency dependence in the centre of the plate by varying skew angle and volume fraction exponent. It can be seen that the skew angle reduce the effect of the nonlinearity, also the increasing volume fraction exponent decrease the nonlinearity. Good agreement between the present results and those found in literature has been achieved. The present study reveals a hardening type of nonlinearity and the nonlinearity in general decreases with the increase in the skew angle and in volume fraction exponent. Further work is needed to investigate the behavior of higher modes, the effects of temperature and the porosity of fully clamped FGSP.

REFERENCES

[1] FA. Fazzolari, E. Carrera, Coupled thermoelastic effect in free vibration analysis of anisotropic multilayered plates and FGM plates by using a variable-kinematics Ritz formulation, European Journal of Mechanics A/Solids, 44, 2014, 157-174.

[2] D. Zhang, Y. Zhou, A theoretical analysis of FGM thin plates based on physical neutral surface, Computational Materials Science, 44, 2008, 716-720

[3] Z. Belabed, M. Houari, A. Tounsi, SR. Mahmoud, O. Anwar Bég, An efficient and simple higher order shear and normal deformation theory for functionally graded material (FGM) plates, Composites: Part B, 60, 2014, 274-283.

[4] T. Prakash, MK. Singha, M. Ganapathi, A finite element study on the large amplitude flexural vibration characteristics of FGM plates under aerodynamic load. International Journal of Non-Linear Mechanics, 47, 2012, 439-447.

[5] N. Duc, P. Cong, Nonlinear post buckling of an eccentrically stiffened thin FGM plate resting on elastic foundations in thermal environments, Thin-Walled Structures, 75, 2014, 103-112.

[6] V. Birman, LW. Byrd, Modelling and analysis of functionally graded materials and structures, Appl. Mech. Rev, 60, 2007, 195-216.

[7] X. Xia, H. Shen, Nonlinear vibration and dynamic response of FGM plates with piezoelectric fiber reinforced composite actuators, Composite Structures, 90, 2009, 254-262.

[8] T. Prakasha, MK. Singhaa, M. Ganapathi, Thermal post buckling analysis of FGM skew plates. Engineering Structures, 30, 2008, 22-32.

[9] A. Boukhzer, K. EL Bikri, R. Benamar, Homogenization technique for non-linear free vibrations analysis of FGM rectangular plates, Advanced Materials Research 2014; 971-973: 516-533.

[10] E. Jaberzadeh, M. Azhari, B. Boroomand, Thermal buckling of functionally graded skew and trapezoidal plates with different boundary conditions using the element-free Galerkin method, European Journal of Mechanics A/Solids, 42, 2013, 18-26.

[11] AK. Upadhyay, KK. Shukla Geometrically nonlinear static and dynamic analysis of functionally graded skew plates, Commun Nonlinear Sci Numer Simulat, 18, 2013, 2252-2279.

[12] J. Yang, S. Kitipornchai, KM. Liew, Large amplitude vibration of thermo-electro-mechanically stressed FGM laminated plates, Comput. Methods Appl. Mech. Engrg, 192, 2003, 3861-3885.

[13] R. Benamar, MMK. Bennouna, RG. White, The effects of large vibration amplitudes on the fundamental mode shape of thin elastic structures, Part II fully clamped rectangular isotropic plates, Journal of Sound and Vibration, 164, 1993, 295-316.

[14] J. Singh, KK. Shukla, Nonlinear flexural analysis of functionally graded plates under different loadings using RBF based meshless method, Engineering Analysis with Boundary Elements, 36, 2012, 1819-1827

[15] A. Gupta, M. Talha, BN. Singh, Vibration characteristics of functionally graded material plate with various boundary constraints using higher order shear deformation theory, Composites Part B, 2016, 1-37.

[16] J. Yang, Hui-Shen Shen, Non-linear analysis of functionally graded plates under transverse andin-plane loads, International Journal of Non-Linear Mechanics, 38, 2003, 467-482.

[17] B. Harras, R. Benamar, RG. White, Experimental and Theoretical Investigation of the Linear and Non-Linear Dynamic Behavior of a Glare 3 Hybrid Composite Panel. Journal of Sound and Vibration, 2, 2002, 281-315.

[18] B. Harras, R. Benamar, RG. White, Geometrically Non-Linear Free Vibration of Fully Clamped Symmetrically Laminated Rectangular Composite Plates. Journal of Sound and Vibration, 4, 2002, 579-619.

[19] B. Harras, R. Benamar, RG. White, Investigation of Non-Linear Free Vibrations of Fully Clamped Symmetrically Laminated Carbon-Fibre-Treinforced PEEK (AS4/APC2) Rectangular Composite Panels, Composite Science and Technology, 62, 2002, 719-727.

[20] Z. Zergoune, B. Harras, R. Benamar, Nonlinear Free Vibrations of C-C-SS-SS Symmetrically Laminated Carbon Fiber Reinforced Plastic (CFRP) Rectangular Composite Plates, World Journal of Mechanics, 5, 2015, 20-32.